A. Paytan and E.T. Gray

Chapter 9

Sulfur Isotope Stratigraphy

Abstract: The sulfur isotopic composition of dissolved sulfate in seawater has varied through time. Distinct variations and relatively high rates of change characterize certain time intervals. This allows for dating and correlation of sediments using sulfur isotopes. The variation in sulfur isotopes and the potential stratigraphic resolution of this isotope system is discussed and graphically displayed.

Chapter Outline

9.1. INTRODUCTION

Sulfur isotope biogeochemistry has broad applications to geological, biological and environmental studies. Sulfur is an important constituent of the Earth's lithosphere, biosphere, hydrosphere and atmosphere, and occurs as a major constituent or in trace amounts in various components of the Earth system. Many of the characteristics of sulfur isotope geochemistry are analogous to those of carbon and nitrogen, as all three elements occur in reduced and oxidized forms, and undergo an oxidation state change as a result of biological processes.

Sulfur as sulfate (SO_4^{2-}) is the second most abundant anion in modern seawater with an average present day concentration of 28 mmol/kg. It has a conservative distribution with uniform SO_4^{2-}/salinity ratios in the open ocean and a very long residence time of close to 10 million years (Chiba and Sakai, 1985; Berner and Berner, 1987). Because of the large pool of sulfate in the ocean, it is expected that the rate of change in either concentration or isotopic composition of sulfate will be small, thus reducing the utility of this isotope system as a viable tool for stratigraphic correlation or dating.

However, as seen in Figures 9.1, 9.2, 9.3 and 9.4, the isotopic record shows distinct variations through time, and at certain intervals, the rate of change and the unique features of the record may yield a reliable numerical age. The features in the record can also be used to correlate between stratigraphic sections and sequences. This is particularly important for sequences dominated by evaporites, where fossils are not abundant or have a restricted distribution range, paramagnetic minerals are rare, and other stratigraphic tools (for example, oxygen isotopes in carbonates) cannot be utilized.

While the potential for the utility of sulfur isotope stratigraphy exists, this system has not been broadly applied. The examples for the application of S isotopes for stratigraphic correlations predominantly focus on the Neoproterozoic and often employ other methods of correlation such as $^{87}Sr/^{86}Sr$ and $\delta^{13}C$ as well (Misi *et al.*, 2007; Pokrovskii *et al.*, 2006; Walter *et al.*, 2000).

The Geologic Time Scale 2012. DOI: 10.1016/B978-0-444-59425-9.00009-3

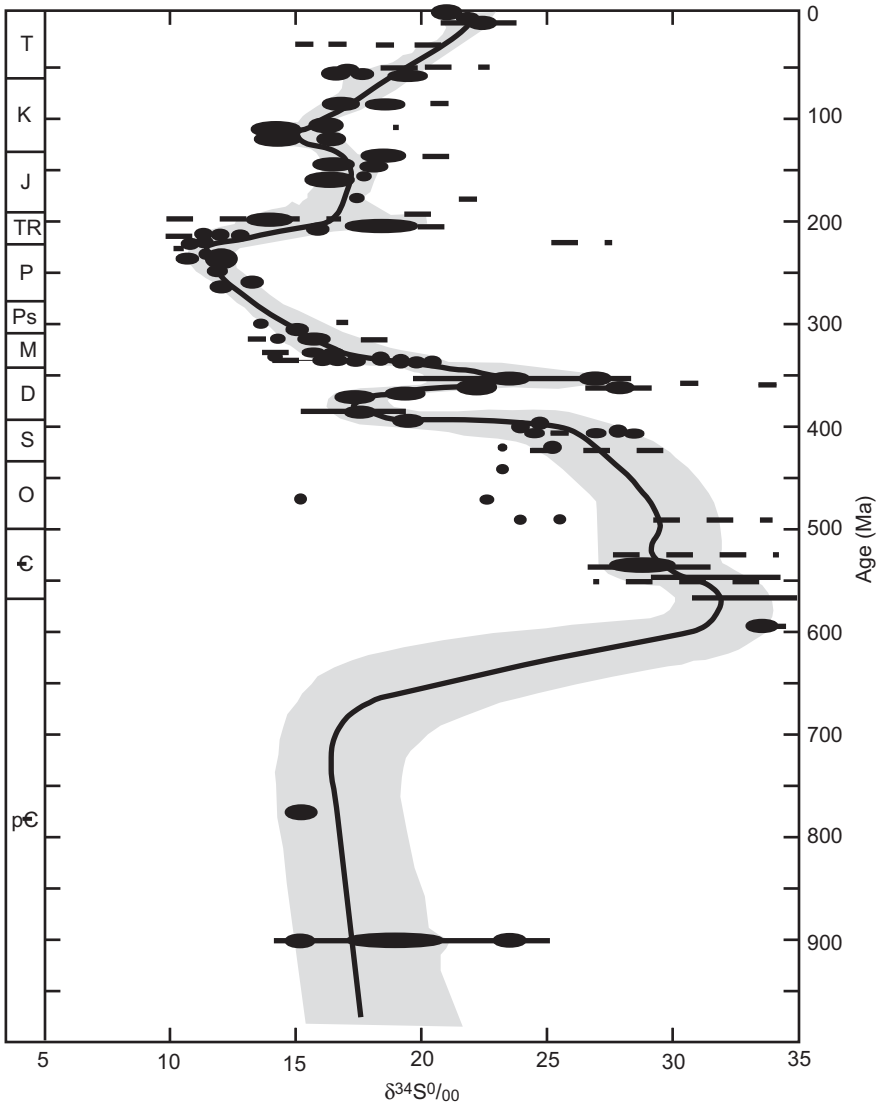

FIGURE 9.1 Evaporite records (Claypool et al., 1980). Solid lines represent data from Claypool et al. and data he compiled from the literature plotted at their most probable age. Dashed lines show the range of all available few analyses for each time interval. The heavy line is the best estimate of $\delta^{34}S$ of the ocean. The shaded area is the uncertainty related to the curve.

It is important to note that the method works only for marine minerals containing sulfate. Moreover, it is crucial that the integrity of the record be confirmed to insure the pristine nature of the record and lack of post-depositional alteration (Kampschulte and Strauss, 2004). In the application of sulfur isotopes it is assumed that the oceans are homogeneous with respect to sulfur isotopes of dissolved sulfate and that they always were so. As noted above, uniformity is expected because of the long residence time of sulfate in the ocean (millions of years) compared to the oceanic mixing time (thousands of years) and because of the high concentration of sulfate in seawater compared to the concentration in major input sources of sulfur to the ocean (rivers, hydrothermal activity, and volcanic activity). Indeed in the present day ocean, seawater maintains constant sulfur isotopic composition (at an analytical precision of $\pm$ 0.2‰) until it is diluted to salinities well below those supportive of fully marine fauna (Rees, 1970; Rees *et al.*, 1978). The main limitation to the broader application of this isotope system for stratigraphy and correlation is the lack of reliable, high-resolution, globally representative isotope records that could be assigned a numerical age scale. As such records become available the utility of this system could expand considerably.

9.2. MECHANISMS DRIVING THE VARIATION IN THE S ISOTOPE RECORD

The chemical and isotopic composition of the ocean changes over time in response to fluctuations in global weathering rates and riverine loads, volcanic activity, hydrothermal exchange rates, sediment diagenesis, and sedimentation and subduction processes. All of these are ultimately controlled

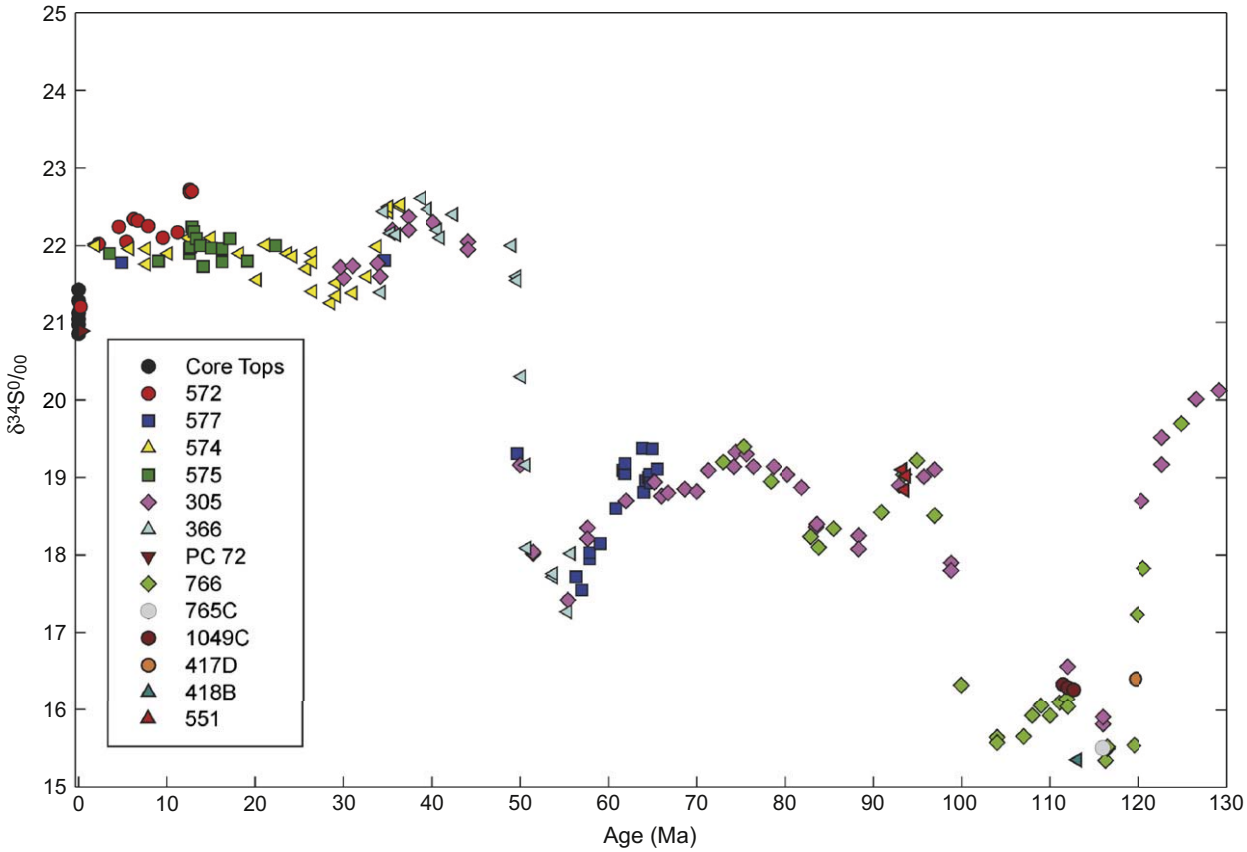

FIGURE 9.2 Seawater sulfate S isotope curve from marine barite for 130 Ma to present (Paytan et al., 2004).

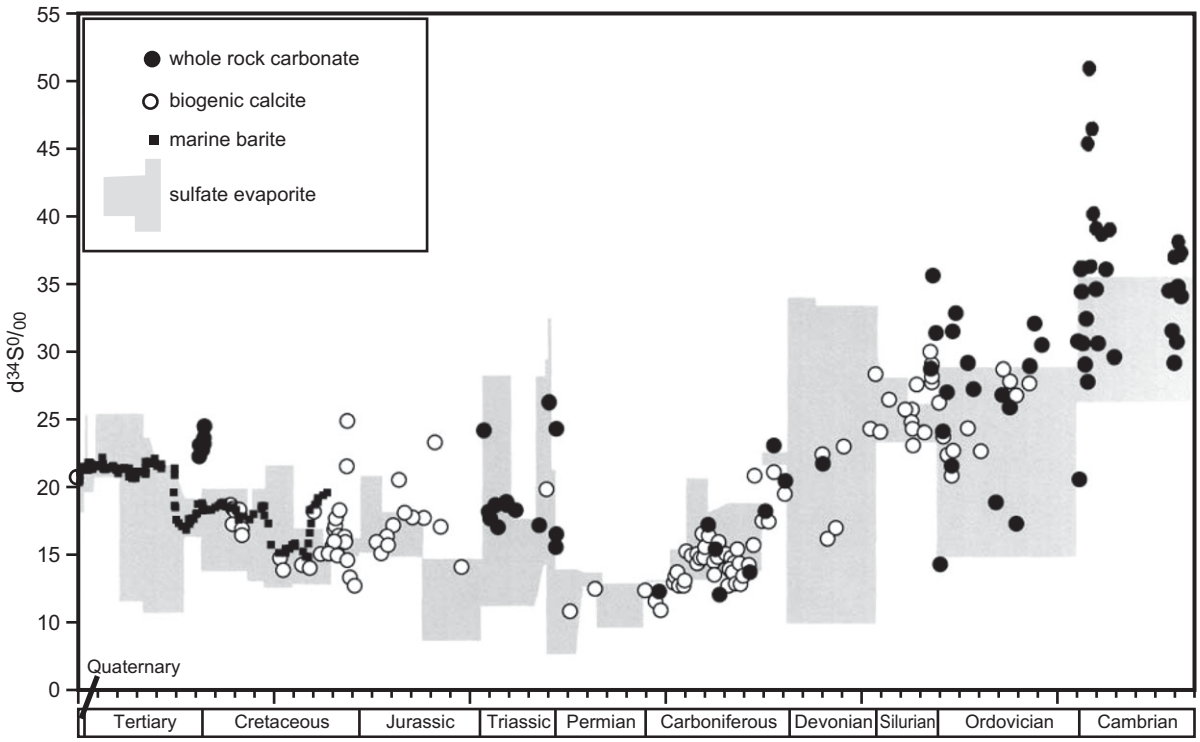

FIGURE 9.3 The carbon associated sulfate record from Kampshulte and Strauss (2004). Evaporite data from Strauss (1997).

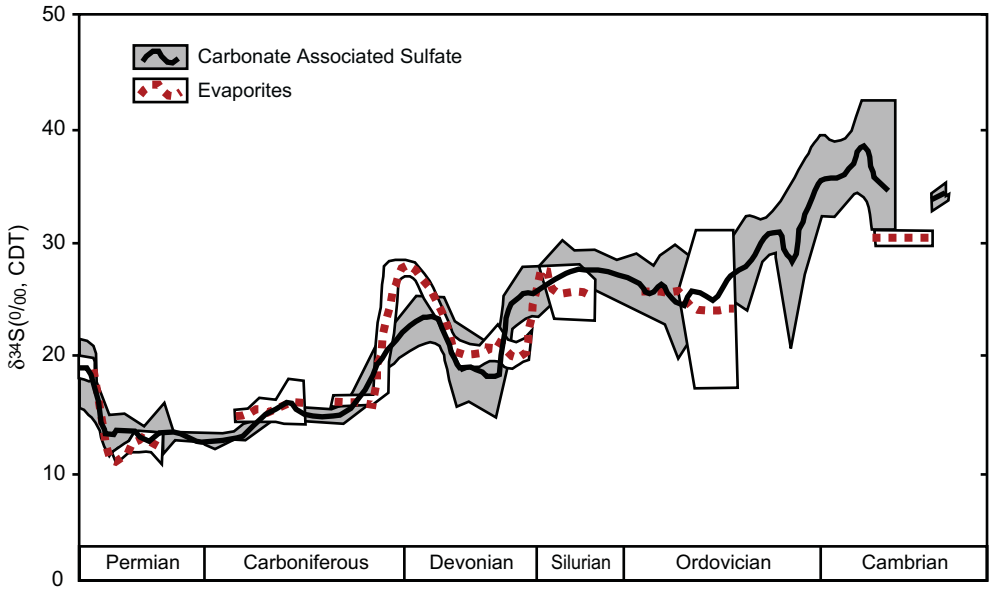

FIGURE 9.4 Compiled record of $\delta^{34}S$ through the Paleozoic. Solid line is the moving mean of carbonate associated sulfate. Dashed line is evaporites. Shaded areas are the respective error. From Kampshulte and Strauss (2004).

by tectonic and climatic changes. Specifically, the oceanic sulfate $\delta^{34}S$ at any given time is controlled by the relative proportion of sulfide and sulfate input and removal from the oceans and their isotopic compositions (e.g., Bottrell and Newton, 2006). S is commonly present in seawater and marine sediments in one of two redox states:

1) in its oxidized state as sulfate and sulfate minerals, and
2) in its reduced form as H_2S and sulfide minerals.

The oceanic sulfate $\delta^{34}S$ record provides an estimate for the relative partitioning of S between the oxidized and reduced reservoirs through time. Changes in both input and output of sulfur to/from the ocean have occurred in response to changes in the geological, geochemical and biological processes (Strauss, 1997; Berner, 1999). These changes are recorded in contemporaneous authigenic minerals which precipitate in the oceanic water column.

Seawater contains a large amount of S ($\sim 40 \times 10^{18}$ mol) that is present, as it has been for at least the past 500 million years, predominantly as oxidized, dissolved sulfate (SO_4^{2-}) (Holser *et al.*, 1988; Berner and Canfield, 1989; 1999). Ancient oceans may have at times had lower sulfate concentrations and thus sulfate residence times may have been shorter (Lowenstein *et al.*, 2001; Horita *et al.*, 2002). The largest input today is from river run-off from the continent. The $\delta^{34}S$ value of this source is variable (0 to 10‰) but typically lower than seawater and depends on the relative amount of gypsum and pyrite in the drainage basin (Krouse, 1980; Arthur, 2000). Volcanism and hydrothermal activity also are small sources of S for the ocean, with $\delta^{34}S$ close to 0‰ (Arthur, 2000). The output flux is via deposition of evaporites and other sulfate containing minerals ($\delta^{34}S_{evaporite} \cong \delta^{34}S_{seawater}$) and sulfides with $\delta^{34}S_{pyrite} \cong -15‰$ (Krouse, 1980; Kaplan, 1983). The typically light isotope ratios of sulfides are a result of the strong S isotope fractionation involved in bacterial sulfate reduction, the precursor for sulfide mineral formation (Krouse, 1980; Kaplan, 1983). This results in the S isotope ratios of seawater sulfate being higher than any of the input sources to the ocean. Seawater sulfate today has a constant $\delta^{34}S$ value of $21.0‰ \pm 0.2‰$ (Rees *et al.*, 1978). It has also been suggested that in addition to changes in the relative rate of burial of reduced and oxidized S the marine $\delta^{34}S$ record has been sensitive to the development of a significant reservoir of H_2S in ancient stratified oceans (Newton *et al.*, 2004). Specifically, extreme changes over very short geological time scales (such as at the Permian–Triassic boundary) along with evidence for ocean anoxia could only be explained via the development of a large, relatively short lived, reservoir of H_2S in the deep oceanic water column followed by oceanic overturning and re-oxygenation of the H_2S.

The evidence that the S isotopic composition of seawater sulfate has fluctuated considerably over time, until recently, was based on comprehensive, though not continuous, isotope data sets obtained from marine evaporitic sulfate deposits and pyrite (Claypool *et al.*, 1980; Strauss, 1993). More recently, marine barite has been used to construct a continuous, high-resolution S curve for the Cenozoic (Paytan *et al.*, 1998) and Cretaceous (Paytan *et al.*, 2004). Methods to analyze the sulfate that is associated with marine carbonate deposits

(carbonate associated sulfate, CAS) have also been developed, and new data sets using these methods are becoming available. Specifically, CAS has been used to reconstruct global change in the sulfur cycle on both long (Kampschulte and Strauss, 2004) and short (Ohkouchi *et al*., 1999; Kampschulte *et al*., 2001) time scales. The new data from barite and from CAS show considerably more detail and fill significant gaps in the former data sets, revealing previously unrecognized structure and increasing the potential for seawater S isotope curves to serve as a tool for stratigraphy and correlation.

9.3. ISOTOPIC FRACTIONATION OF SULFUR

The sulfur isotope fractionation between evaporitic sulfate minerals and dissolved sulfate is approximately 1−2‰ (Thode and Monster, 1965). Experiments and analyses of modern evaporites show values 1.1 ± 0.9‰ heavier than dissolved ocean sulfate (Holser and Kaplan, 1966). Modern barites measured by the SF_6 method averaged 0.2‰ heavier than dissolved ocean sulfate (Paytan *et al*., 1998). Carbonates are also expected to have minor fractionation associated with the incorporation of sulfate. The similarity between the $\delta^{34}S$ value of sulfate minerals and dissolved sulfate means that ancient sulfates can be used as a proxy for the $\delta^{34}S$ value of the ocean at the time that the minerals formed.

Reduced S compounds are mostly produced in association with processes of bacterial sulfate reduction. Dissimilatory reduction (converting sulfate to sulfide) is performed by heterotrophic organisms, particularly sulfate-reducing bacteria. Bacterial sulfate reduction is an energy-yielding, anaerobic process that occurs only in reducing environments (Goldhaber and Kaplan, 1974; Canfield, 2001). Measured fractionations associated with sulfate reduction under experimental conditions range from −20 to −46‰ at low rates of sulfate reduction to −10‰ at high reduction rates. The $\delta^{34}S$ values of sulfides of modern marine sediments are typically around −40‰; however, a wide range from −40‰ to +3‰ is observed. Sulfate reduction and iron sulfide precipitation continues only as long as:

1) sulfate is available as an oxidant,
2) organic matter is available for sulfate-reducing bacteria, and
3) reactive iron is present to react with H_2S.

In the marine environment, neither sulfate nor iron generally limit the reaction. Instead, it is the abundance of easily metabolized carbon that controls the extent of sulfate reduction. The broad range of $\delta^{34}S$ values observed in sulfides from marine sediments results from variable fractionation associated with the different sedimentary settings and environmental conditions during sulfate reduction (temperature, porosity, diffusion rates, etc.) as well as other processes in the S cycle that involve fractionation such as sulfur disproportionation reactions (Canfield and Thamdrup, 1994; Habicht *et al*., 1998).

Assimilatory reduction occurs in autotrophic organisms where sulfur is incorporated in proteins, particularly as S^{2-} in amino acids. Assimilatory reduction involves a valence change from +6 to −2. The bonding of the product sulfur is similar to the dissolved sulfate ion, and fractionations are small (+0.5 to −4.5‰, Kaplan, 1983). The $\delta^{34}S$ value of organic sulfur in extant marine organisms incorporated by assimilatory processes is generally depleted by 0 to 5‰ relative to the ocean.

The wide array of environmental conditions that affect the fractionation, together with the broad range of S isotopic values of sulfide minerals at any given time, and post-depositional alteration of assimilatory S into organic matter, limit the utility of sulfites and S in old organic matter as tools for stratigraphy and correlation, since measured values may not be representative of a global oceanic signature.

9.4. MEASUREMENT AND MATERIALS FOR SULFUR ISOTOPE STRATIGRAPHY

9.4.1. Isotope Analyses

There are four stable isotopes of sulfur. The isotopes that are commonly measured are ^{34}S and ^{32}S, as these are the two most abundant of the four. In most but not all samples, the sulfur isotopes are present in constant ratios to each other, thus the others could be easily computed (but see Farquhar *et al*., 2000). All values are reported as $\delta^{34}S$ relative to the Cañon Diablo Troilite (CDT) standard (Ault and Jensen, 1963) using the accepted delta notation. Due to scarcity of the CDT standard, secondary synthetic argentite (Ag_2S) and other sulfur-bearing standards have been developed, with $\delta^{34}S$ values being defined relative to the accepted CTD value of 0‰. Samples are converted to gas (SO_2 or SF_6) and analyzed on a gas ratio mass-spectrometer. Analytical reproducibility is typically ±0.2‰.

9.4.2. Materials for S Isotope Analysis

9.4.2.1. Evaporites

Records of oceanic sulfur isotopes through time were originally reconstructed from the analyses of marine evaporitic sulfate minerals (Holser and Kaplan, 1966; Claypool *et al*., 1980). Evaporites contain abundant sulfate and their formation involves minimal and predictable fractionation, thus they are suitable archives for this analysis. Claypool *et al*. (1980) presented the first compilation of the secular sulfur isotope record of seawater for the Phanerozoic (Figure 9.1) and their work provides the basis for our understanding of the sulfur isotope record. However, as a result of the sporadic nature of evaporite formation through geological time this record is not continuous. Moreover, evaporites are hard to date precisely due to the limited fossil record within these sequences; thus

the stratigraphic age control on the evaporitic-based sulfur isotope record is compromised.

9.4.2.2. Barite

Like evaporites, the $\delta^{34}S$ of barite is quite similar to that of the sulfate in the solution from which it precipitated. Marine barite precipitates in the oceanic water column and is relatively immune to diagenetic alteration after burial — thus it records the changes in the sulfur isotopic composition of seawater through time (Paytan *et al.*, 1998, 2004). Moreover, high-resolution, well dated and continuous records can be developed as long as barite-containing pelagic marine sediments are available (Paytan *et al.*, 1993). It must be stressed that reliable seawater sulfur isotope records can only be derived from marine (pelagic) barite and not diagenetic or hydrothermal barite deposits (see Eagle *et al.*, 2003 and Griffith and Paytan 2012 for more details). A sulfur isotope curve was obtained from pelagic marine barites of Cretaceous and Cenozoic age with unprecedented temporal resolution (Paytan *et al.*, 1998, 2004; Figure 9.2). The high-resolution curve shows some very rapid changes that could be instrumental for stratigraphic applications.

9.4.2.3. Substituted Sulfate in Carbonates

Sulfur is a ubiquitous trace element in sedimentary carbonates (e.g., carbonate associated sulfate, CAS). Concentrations range from several tens of ppm in inorganic carbonates to several thousand ppm in some biogenic carbonates (Burdett *et al.*, 1989; Kampschulte *et al.*, 2001; Lyons *et al.*, 2004). While the mechanism of sulfate incorporation into carbonates is not fully understood, CAS is incorporated with little fractionation thus recording seawater ratios. Carbonates offer an attractive method for refining the secular sulfur curve, because of their abundance in the geological record, ease of dating and relatively high accumulation rates. Indeed, a record for Phanerozoic seawater sulfur isotopes based on CAS has been compiled and published (Kampschulte and Strauss, 2004; Figure 9.3). Extreme caution must, however, be exercised in extracting CAS from samples and interpreting the sulfur isotope data obtained because carbonates are highly susceptible to post-depositional alteration and secondary mineral precipitation which can obliterate the record. The degree of modification can be assessed by obtaining multiple records from distinct locations (or mineral phases) for the same time interval and construction of secular trends (Kampschulte and Strauss, 2004).

9.5. A GEOLOGICAL TIME SCALE DATABASE

9.5.1. General Trends

The current sulfur isotope records include data sets from the Cambrian to the present (Figures 9.4 and 9.5). While the

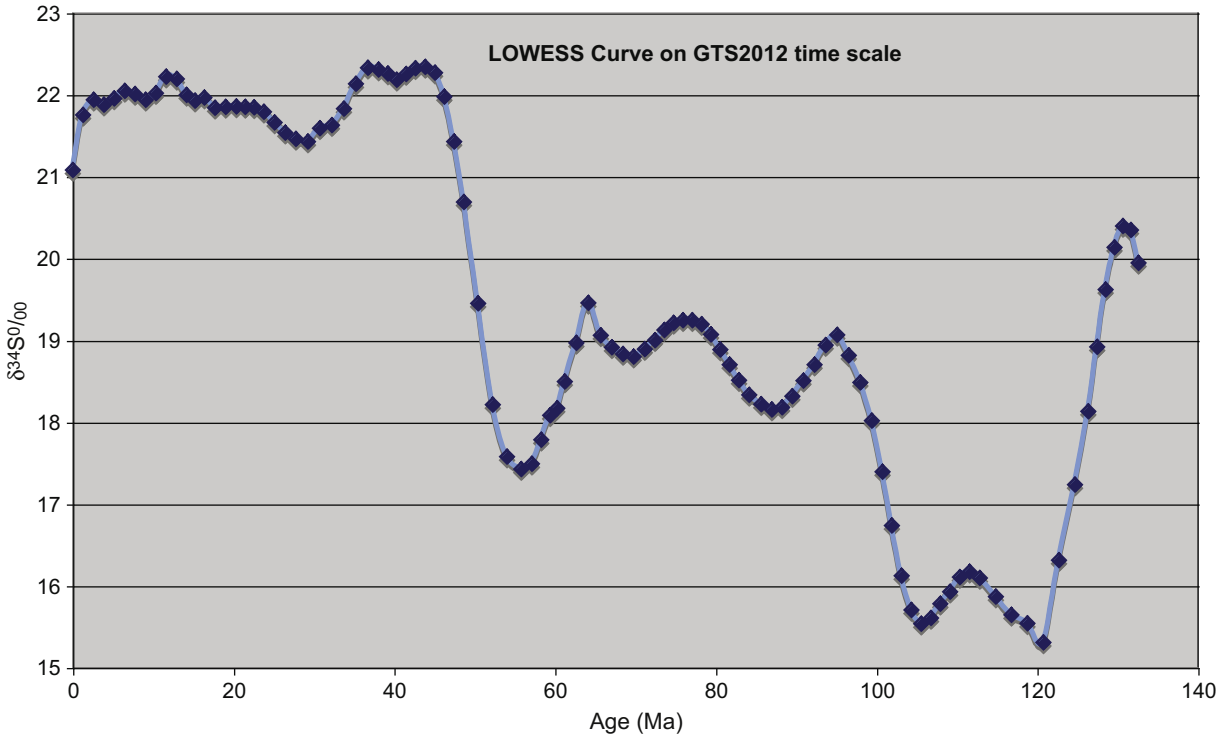

FIGURE 9.5 LOWESS curve for the last 130 million years generated from marine barite data (Paytan et al., 2004); see also Table 9.1.

focus of most studies is on shorter time scales and the methods that are used are varied, the overlap agreement among published records and a few long-term studies serve to give a comprehensive view of the sulfur isotope record for the Phanerozoic. Three long-term records have been compiled, two based on evaporites (Claypool *et al.*, 1980; Strauss, 1997) and one based on carbonate associated sulfate (Kampschulte and Strauss, 2004).

A general trend can be seen in these records. In the Cambrian, the average $\delta^{34}S$ value is 34.8 ± 2.8‰ in the CAS record (Kampschulte and Strauss, 2004) and around 30‰ in the evaporite record (Claypool, *et al.*, 1980; Strauss, 1997). These relatively high values are sustained through the Cambrian in the CAS record, ending with anomalously high $\delta^{34}S$ values at the Cambrian/Ordovician boundary. After this point, the $\delta^{34}S$ decreases steadily through the remainder of the Paleozoic, reaching a minimum at the Permian/Triassic boundary with an average value of 13.2 ± 2.5‰. A similar but less time constrained decrease is seen in the evaporite record.

Through the Mesozoic, the $\delta^{34}S$ values are generally lower than in the Paleozoic, ranging between 14 and 20‰. The $\delta^{34}S$ values increase quite rapidly, from 13.2 ± 2.5‰ at the Permian/Triassic boundary to 17‰ in the Jurassic, and decrease again to about 15‰ in the Early Cretaceous (Claypool *et al.*, 1980; Strauss, 1997; Kampschulte and Strauss, 2004). The value at the Cretaceous is about 19‰ but two distinct excursions towards lower values are seen: one at ~120 Ma and the second at ~90 Ma (Paytan *et al.*, 2004). A decrease in $\delta^{34}S$ values from ~20‰ to 16‰ is seen in the Paleocene before climbing sharply in the Early to Middle Eocene to the near modern value of 21‰ where it remains steady for the remainder of the Cenozoic (Paytan *et al.*, 1998).

These broad trends can be useful in obtaining very general stratigraphic information (e.g., typically only at the epoch scale) but are not applicable for age assignments at resolution better than tens of millions of years.

9.5.2. Time Boundaries

Strauss (1997) reviewed secular variations in $\delta^{34}S$ across time boundaries characterized by profound biological or geological changes. Due to the paucity of evaporite data, all these time boundary studies have used data obtained from sedimentary sulfides. The premise behind the study of S isotope excursions at age boundaries is based on the expected perturbations in the biosphere which may impact sulfate reduction rates. During a catastrophic event, where productivity plunges, the $\delta^{34}S$ values of the oceans are expected to decrease because of a reduction in organic matter availability, leading to lower sulfate reduction. The subsequent biological radiations should have the opposite effect. Accordingly, the $\delta^{34}S$ values of the oceans should first decrease across a time boundary associated with a catastrophic extinction or major ecosystem reorganization, and then increase during the period of recovery. The magnitude of the effect is related to the intensity of the extinction event, the rate of recovery, and the size of the oceanic sulfur reservoir.

Four extinction events have been studied (see Strauss, 1997 for references): the Precambrian–Cambrian, the Frasnian–Famennian, the Permian–Triassic, and the Cretaceous–Tertiary boundaries. Of these, only the Permian–Triassic event shows the expected sulfur trend. Fluctuations occur at the other boundaries, but no secular (globally concurrent) variations have been observed (see also Newton *et al.*, 2004). In part, the reason for the inconsistent results between sections and between extinction events may be related to the inherent problems of analyzing sulfides instead of sulfates and the multitude of controls impacting the isotopic composition of sulfides. Therefore, local effects may mask any global sulfur variations.

9.5.3. Age Resolution

Age resolution of the S isotope curve varies with the type of data comprising the record and the specific objectives for the various studies producing the data. The older sections compiled from evaporite and CAS data have a lower resolution because of the scarcity of evaporites and because CAS depends on the integrity of the carbonates and fossils used for reconstruction, which, in many locations, are subjected to extensive post-depositional alteration. In addition, large temporal gaps between samples make it difficult to correlate between sites and thus make exact age determinations challenging. Despite these limitations, robust records exist for specific time periods and the confidence within each such time interval is considerably improved over the earlier evaporite records. The age resolution of records based on barite are much better, but so far barite has been recovered predominantly from pelagic sediments, limiting its applicability to the last 130 Ma.

The Phanerozoic evaporite record, compiled by Claypool *et al.* (1980) with further work done by Strauss (1997), has several characteristics that make it difficult to use for S stratigraphy. First, the record has large gaps in it that leave long periods of time unaccounted for. In Claypool *et al.* (1980), a best estimate curve was visually approximated to combine and extrapolate between disparate data sets; however this smooths over finer fluctuations that may be present. Second, the absolute S isotope values recorded at each time point range considerably, confounding the issue. The range of $\delta^{34}S$ values within each time interval is approximately 5‰ for most of the data sets which makes pinpointing an age from a stratigraphic perspective difficult since in many cases the broad fluctuations that occur over time are within ±5‰ (Figure 9.1). Third, the ages used for each sample are approximate due to the scarcity of fossils in sections used to compile the isotope curves. Even in the evaporite record from Strauss

(1999) that derives its ages after Harland *et al*. (1990), the age uncertainty spans more than 10 million years depending on the segment (or specific time range), which makes it difficult to use these data for stratigraphic correlation (Strauss, 1999).

The S isotope record derived from CAS is more robust (Figure 9.3). The record is consistent with the evaporite data in the broad strokes (Figure 9.4) but a better constraint on the ages of the samples is possible. The data sets presented in Kampschulte and Strauss (2004) and references therein show a record for the Phanerozoic that reduces the uncertainty in age and S isotope values considerably from those associated with evaporites. The CAS samples were taken from stratigraphically well-constrained biogenic calcites (using the time scale of Harland *et al*., 1990) with a resolution of 1−5 million years within data sets. However, the data sets analyzed are not continuous, leaving gaps that, while not as glaring as those in the evaporite record, still limit the accuracy of a smooth curve and may miss finer details. The CAS data that represent older ages have a wider range of S isotope values than that of more recent (younger) samples. For example, a "scatter" of ±10‰ and even up to 20‰ in the Cambrian and Ordovician is seen for samples with similar ages. More recent samples have narrower ranges, from 5‰ to 10‰, and thus would be more useful for stratigraphy, although in some places the low temporal resolution still makes it difficult to distinguish noise from trend (Kampschulte and Strauss, 2004).

The data compiled and presented in Kampschulte and Strauss (2004) is presented as a moving average to create a continuous curve (Figure 9.4). The effect is to smooth out the observed variation that then make it difficult to assess the error associated with both the isotope data set (e.g., $\delta^{34}S$) and the age resolution. This makes it difficult to resolve trends and compare the data with other records or to use the curve for precise sample age determination. The smoothed curve of Kampschulte and Strauss (2004) can, however, be used to assess the utility of certain sections (age intervals) of the record for dating using S stratigraphy, but because the specific data sets used to produce the smooth curve were not available to us, evaluation of age resolution or a detailed statistical LOWESS fit (McArthur *et al*., 2001) for derivation of numeric ages using the CAS record cannot be compiled at this time.

The marine barite record presented by Paytan *et al*. (1998, 2004) is derived from ocean floor sediment. The current record goes back ~130 Ma. The barite-based S isotope curve provides a record with a resolution of less than 1 million years with very few gaps. The age of the samples is constrained by biostratigraphy and Sr isotopes and typically has an error of less than 100 000 years. The continuous and secular (based on data from multiple sites for each time interval) nature and the high resolution of this record illuminate finer features that are missed in the lower resolution evaporite and CAS records. The record also has a narrower range of S isotope values for each time point, further constraining the curve. These features make it the most robust of the three available records thus far and the most useful for stratigraphy, for the periods it covers. This record serves to illustrate the potential use of S isotopes for stratigraphy and, as more such detailed high-resolution secular records (e.g., based on coherent data from multiple locations and settings) become available for different geological periods, S isotope stratigraphy can be more widely utilized. At the moment, the limited availability of continuous high-resolution secular data and the need for updated and better constrained ages for previously published records are the biggest obstacles to using sulfur isotopes as a stratigraphic tool.

9.5.4. Specific Age Intervals

While the current S record of the Phanerozoic is not ideal for stratigraphic applications as discussed above, there is still potential for using S as a stratigraphic tool for certain time intervals within the Phanerozoic. The time periods best suited to dating are those that are distinguished by rapid changes in $\delta^{34}S$. Identifying smaller fluctuations on the "plateaus" of the isotope curve is difficult because of the limited temporal resolution, and the relatively large error in the $\delta^{34}S$ compared to the small fluctuations. These limitations make the potential use of fine features for stratigraphic and correlation purposes impossible at this stage.

At this time, the most useful record for S stratigraphy applications is the marine barite curve that extends back to 130 Ma. The distinct features that appear in this high-resolution curve show five time periods with relatively abrupt changes in $\delta^{34}S$ that could lead to precise dating: 130−116 Ma, 107−96 Ma, 96−86 Ma, 83−75 Ma, and 65−45 Ma. Resolving ages during periods of smaller fluctuations is possible but would likely necessitate a much larger data set in order to match multiple points and avoid offsets between data from distinct sites. The plateaus, notably from ~30 Ma to about 2 Ma, where the S isotope values do not significantly change are not useful because there are few features that can be teased out and distinguished from sampling and analytical error.

Below we present the trends in the $\delta^{34}S$ isotope data for each time period, together with a brief discussion of the utility of the data for stratigraphy. Kampschulte and Strauss (2004) showed that the Phanerozoic CAS record is consistent with, and better constrained temporally than, the evaporite record. For this reason, the trends discussed below will rely on the CAS record from the Cambrian to the Jurassic (Kampschulte and Strauss, 2004, and references therein) and the barite record from Paytan *et al*. (1998, 2004) from the Cretaceous to the present, unless otherwise specified.

9.5.4.1. Cambrian

The $\delta^{34}S$ data from the Cambrian consists of two sets of carbonate associated sulfate records (Kampschulte and

Strauss, 2004). The data are from 33 whole rock samples in the Kuljumbe section in northwestern Siberia. Twelve samples are from the lower Cambrian with an average $\delta^{34}S$ value of 34.5 ± 2.8‰, and the remaining 21 are from the middle and upper Cambrian − from 527.8−510.3 Ma − showing $\delta^{34}S$ within the same range as the lower Cambrian. The data show a distinct excursion that maximizes at 50.1‰, although it is unclear at this time if these latter values reflect open ocean seawater sulfate or if the integrity of these samples was compromised.

The age resolution that can be theoretically obtained using the moving mean curve is 2.0 myr from 535 to 525 Ma and 2.8 myr from 525 to 511 Ma (but note that the curve averages values over 5 myr) (Kampschulte and Strauss, 2004). When looking at the raw data, one sees that there is a significant age gap between the two time periods sampled that is smoothed over in the moving mean. Additionally, while the $\delta^{34}S$ values in both data sets are relatively high (>30‰) and can be used to identify samples of Cambrian age, the range of values is similar for both sets and thus, without a larger data set that fills in the gaps, distinguishing between older and younger samples within the Cambrian may be difficult. Moreover, it is important to verify the global nature of these isotope values using data from other distinct sites such that post-deposition alteration of the isotope values can be ruled out.

9.5.4.2. Ordovician

The CAS record in the Ordovician is composed of 16 samples. The temporal resolution of the record is between 1 and 8 million years with the older samples predominantly ~4 million years apart and the younger samples 1 million years apart. The $\delta^{34}S$ values were determined from whole rock in 15 of these samples, and for 12 of them brachiopod shells were also used. The record shows a decrease from a moving mean of 30‰ in the lower Ordovician to 24‰ in the uppermost Ordovician (Kampschulte and Strauss, 2004).

The wide range of the measured $\delta^{34}S$ values (15−30‰) throughout the period complicates the picture. Without a higher resolution data set, it is impossible to distinguish whether the broad range represents real fluctuations and the lower values (15‰) are a true minimum. Specifically, when considering the time resolution of the recorded, values of 15‰ and ~30‰ appear to occur within the same time frame rendering the use of such records unreliable. However, on a broader scale, the moving average of $\delta^{34}S$ values, which plateaus around 24‰ at ~475 Ma and remains at that level up to the Ordovician/Silurian boundary, can be distinguished from other time periods.

9.5.4.3. Silurian

The Silurian shows a continued trend of decreasing $\delta^{34}S$ values with a range from 35.6‰ to 21.5‰ in the CAS record in 15 brachiopod shells and 17 whole rock samples over 30 myr (Kampschulte and Strauss, 2004). The Ordovician/Silurian boundary exhibits the higher values (30−35‰) which drop by 1−2‰ in the Early Silurian. Following is a narrower range of S isotope values from ~24−28‰ and the moving mean shows a plateau in the record. The running mean seems to smooth away the slight downward trend seen in the raw data. Having the mean at odds with the trend in the raw data makes the curve from this section within the Silurian difficult to use for stratigraphic dating, because there is no good way to resolve the inconsistencies without a more complete record. Nevertheless, the range from ~24−28‰ is distinctive to the Late Ordovician and Silurian.

9.5.4.4. Devonian

A total of 18 samples comprise the record for the Devonian. $\delta^{34}S$ values in the Devonian show a downward trend, decreasing from ~25‰ in the Late Silurian to ~19‰ in the lower middle Devonian. The steep slope of the curve from 408−395 Ma make it useful for stratigraphy, specifically a 6‰ change over 13 million years and an isotope analytical error of 0.2‰ can yield an age resolution in the range of 0.5 million years. In the second section, from 395−381 Ma, the curve plateaus; the moving average remains around 18.8−19.2 per mil. The remainder of the Devonian exhibits a distinctive peak with $\delta^{34}S$ increasing from 23‰ in the Frasnian age of the Late Devonian (371 Ma) to a maximum of 26.9‰ (Kampschulte and Strauss, 2004). The age resolution of the data set varies between 1 and 4 myr with a gap of 8 million years over the Devonian/Carboniferous boundary. The shape of the curve makes this section distinct and thus potentially useful for stratigraphy; however, the moving mean currently smooths the data. The range of values in the raw data, along with the paucity of data that was used to construct the curve in the Early Devonian, mean that this feature could only be used if a large data set was available that could be used to verify and refine the overall pattern.

9.5.4.5. Carboniferous

The Carboniferous is also characterized by a decrease in the CAS data from ~20‰ in the Early Carboniferous (Mississippian) to ~15‰ at 334 Ma where it remains until decreasing to around 12‰ in the Late Carboniferous (Pennsylvanian; Kampschulte and Strauss, 2004). The age resolution of the record, based on the moving mean, ranges from 5.6 myr from 362 to 334 Ma in the Mississippian and 3−4 myr for the remainder of the period. The overall range of values in the raw data is narrower than for other sections, which makes distinguishing between noise and trend easier. However, the values plateau from 342.8 Ma to 309.2 Ma and leave only the beginning and end of the period significantly distinguishable for stratigraphic correlation. Thus, there is a potential for stratigraphic applications for the Early and Late Carboniferous, provided the available data is indeed representative of

global trends. The potential age resolution for these time intervals is in the range of about 1 million years (5‰ change over about 20 million years).

9.5.4.6. Permian

The Permian record maintains the low $\delta^{34}S$ values that characterize the end of the Carboniferous, around 12‰. This value is seen in the 16 samples analyzed for the Permian (Kampschulte and Strauss, 2004). This overall $\delta^{34}S$ value is distinctive for the period and is useful for dating it as a whole, but the plateau in the record does not lend itself to more precise stratigraphic dating or correlation within the Permian.

The Permian/Triassic boundary has been sampled at the higher resolution of 1 myr (Kramm and Wedepohl, 1991; Scholle, 1995; Newton *et al*., 2004; Algeo *et al*., 2007; Gorjan *et al*., 2007) and shows distinct fluctuations that are useful stratigraphically (see below).

9.5.4.7. Triassic

The transition from the Paleozoic to the Mesozoic is marked by an abrupt shift in sulfur isotope values from the low 12‰ value of the Late Permian to 29.7‰ in the lower Triassic. This excursion is short and the rest of the Triassic maintains values in the narrower range of 17.3 to 19.7‰ until the uppermost Triassic where short-term fluctuations between 11.1‰ and 24.3‰ occur (Kampschulte and Strauss, 2004).

The excursion at the Permian–Triassic boundary to 29.7‰ is distinctive, but the later fluctuations are more difficult to distinguish since the temporal trends of the data are not easily resolved and the temporal resolution is low. The age resolution for the majority of the Triassic is from <1 myr at the Permian–Triassic boundary to 4 million years for the rest of the record, with a gap from 234.7 to 224.7 Ma. The excursion at the Permian–Triassic boundary of up to 17‰ over only a few million years allows for age resolution of less than 100 000 years; however a more coherent and high-resolution curve should be produced prior to such application. Regardless, provided the global nature of the trend is robust, the distinct excursion at this time interval could clearly be used for correlation between sections.

9.5.4.8. Jurassic

The Jurassic $\delta^{34}S$ values range from 14.2 to 18.0‰ with two exceptional excursions. The first occurs in the lower middle Jurassic with a $\delta^{34}S$ value of 23.4‰. The second occurs in the upper middle Jurassic with a $\delta^{34}S$ value of 20.7‰ (Kampschulte and Strauss, 2004). The potential for detailed stratigraphy exists; however, the majority of the data, 18 samples, is poorly constrained with an error of ±31.2 Ma that needs to be resolved before these samples can be used for detailed stratigraphy (Kampschulte and Strauss, 2004).

9.5.4.9. Cretaceous

The Cretaceous record (Figure 9.2) derived from marine barite by Paytan *et al*. (2004) is a continuous record that has a resolution of less than 1 million years. A negative shift from ~20 to15‰ occurs from 130 to 120 Ma, remaining low until 104 Ma when it rises to ~19‰ over 10 million years. There is a small minimum at 88 Ma with a value of 18.0‰, returning to values of 18 to 19‰ at ~80 Ma for the remainder of the period.

These results generally agree with the CAS data from Kampschulte and Strauss (2004). This record and the observed fluctuations further illuminate variations that can be seen when the finer scale rather than the smoothed record is available. The finer detail and the observed changes that occur particulary in the beginning of this period make this record useful for stratigraphy and will be discussed later in the chapter.

9.5.4.10. Cenozoic

A high-resolution barite curve for the Cenozoic (Figure 9.2) with an age resolution of <1 myr shows $\delta^{34}S$ values of ~19‰ at the Cretaceous/Tertiary boundary which drop precipitously to ~17‰ at the Paleocene/Eocene boundary. Following this minimum a relatively rapid rise to ~22‰ in the Early to Mid Eocene is observed and this value is maintained until the Pleistocene. The decrease and increase observed between 65 to 47 Ma are useful for stratigraphic purposes (see below). A possible decrease of about 1‰ over the last 2 million years is also evident but is defined by relatively few samples.

9.6. A DATABASE OF S ISOTOPE VALUES AND THEIR AGES FOR THE PAST 130 MILLION YEARS USING LOWESS REGRESSION

At this early stage of development in S isotope stratigraphy, we can see the general trends for the record throughout the Phanerozoic. These trends and values can be used for broad age assignments and correlations at distinct intervals with defined excursions (e.g., the Permian–Triassic boundary). The goal of developing a LOWESS regression curve for S isotopes and accompanying look-up tables has not yet been realized. Currently, the limits to developing such tables include the availability of raw data to construct secular trends, the unknown error associated with age assignments, and gaps in the data sets. The potential for using LOWESS regression, however, can be illustrated by the marine barite data sets over the Cretaceous and Cenozoic (Figure 9.5). The LOWESS regression curve shown in Figure 9.5 was produced according to McArthur *et al*. (2001).

Based on the LOWESS curve we calculated the age resolution associated with the five age intervals that exhibit abrupt changes in $\delta^{34}S$: 130–116 Ma, 107–96 Ma,

TABLE 9.1 Preliminary Look-Up Table for the Data set of Figure 9.5.

Age	$\delta^{34}S$	Age	$\delta^{34}S$	Age	$\delta^{34}S$	Age	$\delta^{34}S$	Age	$\delta^{34}S$
0.00	21.13	28.45	21.43	53.70	17.59	85.60	18.26	120.13	16.75
0.00	21.13	29.06	21.46	53.80	17.58	88.41	18.27	120.26	16.95
0.24	21.21	30.92	21.57	55.40	17.42	90.12	18.47	120.39	17.15
0.40	21.27	31.00	21.57	55.45	17.43	91.00	18.58	120.50	17.32
0.97	21.47	32.50	21.70	55.50	17.44	92.26	18.78	120.63	17.52
1.55	21.67	33.36	21.90	55.80	17.52	93.00	18.89	120.70	17.63
1.94	21.80	33.62	21.96	56.53	17.70	93.40	18.96	120.98	17.83
2.28	21.92	33.90	22.03	57.20	17.87	93.50	18.97	121.27	18.03
3.50	21.93	34.10	22.07	57.90	18.04	93.60	18.97	121.55	18.23
3.58	21.93	34.40	22.14	58.00	18.05	93.80	18.97	121.83	18.43
4.55	21.94	34.50	22.17	59.60	18.19	95.00	18.98	122.11	18.63
4.85	21.95	34.95	22.27	60.28	18.39	95.78	18.98	122.40	18.83
5.40	21.98	35.20	22.28	60.96	18.59	96.52	18.78	122.68	19.03
5.74	22.00	35.40	22.29	61.64	18.79	97.00	18.65	122.81	19.12
5.90	22.01	35.80	22.30	62.20	18.96	97.34	18.45	123.58	19.32
6.23	22.03	36.00	22.31	62.40	18.97	97.68	18.25	124.35	19.52
6.68	22.05	36.31	22.32	62.49	18.98	98.02	18.05	125.00	19.69
7.64	22.02	37.50	22.37	62.50	18.98	98.36	17.85	126.65	19.89
7.85	22.01	38.70	22.28	63.86	19.05	98.70	17.65	126.65	19.89
9.00	21.97	39.00	22.26	64.01	19.06	98.87	17.55	128.22	20.09
9.50	22.00	39.50	22.22	64.21	19.07	99.29	17.35	129.17	20.21
10.10	22.04	40.70	22.25	64.32	19.08	99.72	17.15		
11.17	22.11	41.00	22.25	64.58	19.10	100.00	17.02		
12.40	22.02	42.50	22.25	64.69	19.10	100.68	16.82		
12.49	22.01	45.30	22.11	64.69	19.10	101.36	16.62		
12.50	22.01	45.95	21.91	64.75	19.11	102.04	16.42		
12.54	22.01	46.59	21.71	64.97	19.07	102.72	16.22		
12.60	22.00	47.10	21.55	65.17	19.03	103.39	16.02		
12.77	21.99	47.39	21.35	65.23	19.02	104.00	15.84		
12.78	21.99	47.69	21.15	65.53	18.97	107.00	15.79		
13.00	21.98	47.98	20.95	66.02	18.89	108.00	15.87		
13.27	21.96	48.28	20.75	66.75	18.77	109.00	15.95		
13.72	21.92	48.57	20.55	68.65	18.84	110.00	16.05		
14.05	21.93	48.87	20.35	70.00	18.94	111.10	16.17		
14.95	21.94	49.10	20.19	71.31	19.03	111.50	16.21		
14.98	21.94	49.31	19.99	73.00	19.16	111.90	16.09		

(*Continued*)

TABLE 9.1 Preliminary Look-Up Table for the Data set of Figure 9.5.—cont'd

Age	$\delta^{34}S$	Age	$\delta^{34}S$	Age	$\delta^{34}S$	Age	$\delta^{34}S$	Age	$\delta^{34}S$
16.20	21.96	49.51	19.79	74.19	19.20	112.00	16.07		
17.04	21.92	49.70	19.61	74.40	19.21	112.70	15.87		
18.13	21.86	49.91	19.41	75.33	19.24	112.70	15.87		
19.00	21.85	50.00	19.32	75.62	19.23	113.00	15.78		
20.14	21.85	50.20	19.13	76.43	19.19	115.97	15.61		
21.08	21.86	50.41	18.93	78.40	19.08	116.00	15.60		
22.20	21.88	50.61	18.73	78.75	19.06	116.30	15.56		
23.55	21.81	50.70	18.64	80.32	18.92	116.50	15.53		
24.14	21.78	50.80	18.55	81.78	18.72	118.06	15.73		
24.60	21.75	51.27	18.35	81.97	18.69	119.60	15.93		
24.80	21.74	51.74	18.15	83.00	18.51	119.73	16.13		
25.68	21.70	52.00	18.03	83.63	18.39	119.80	16.24		
26.36	21.66	52.47	17.83	83.70	18.38	119.93	16.44		
28.16	21.46	52.82	17.68	83.90	18.34	120.00	16.55		

96–86 Ma, 83–75 Ma, and 65–45 Ma. Age resolutions are 0.5 myr, 0.7 myr, 2.6 myr, 2.1 myr, and 1.5 myr respectively based on the data and an analytical error of 0.2‰. From this curve we also generated a preliminary look-up table for the data set (Table 9.1).

9.7. USE OF S ISOTOPES FOR CORRELATION

S isotopes have not been widely used as the sole stratigraphic tool for dating samples. The few examples in the literature of S isotopes used for dating and correlation all also use other methods such as $\delta^{13}C$ and $^{87}Sr/^{86}Sr$ at the same time (Walter *et al.*, 2000; Pokrovskii *et al.*, 2006; Misi *et al.*, 2007). Some studies, particularly those focused on the Permian/Triassic boundary (Scholle, 1995; Kramm, *et al.*, 1991; Algeo, *et al.*, 2007; Gorjan, *et al.*, 2007), use $\delta^{13}C$, $^{87}Sr/^{86}Sr$, biostratigraphy, paleomagnetism, and other methods to correlate the S isotope records and use the S data to investigate the causes and consequences of various biogeochemical cycles across the boundary. Nevertheless, the secular and defined trend in the S isotope record at this time interval could be used for correlation and age

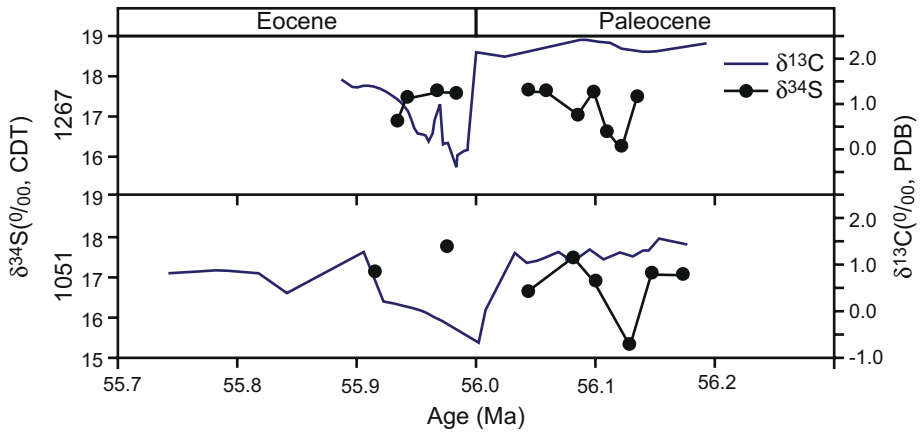

FIGURE 9.6 $\delta^{13}C$ and seawater $\delta^{34}S$ isotope records over the Paleocene Eocene Thermal Maximum in the Atlantic Ocean. Site 1051 is in the North Atlantic and Site 1267 is in the South Atlantic. The S isotope record was used to correlate the two sites when the $\delta^{13}C$ record was insufficient. Ages were determined by biostraigraphy (Gray, 2007).

determination in the future where methods other than S isotopes are not available or to refine age assignments based on other records.

The utility of using S isotopes for correlation between sites is illustrated in Figure 9.6 from Gray (2007). This study focuses on the Paleocene Eocene Thermal Maximum at 56 Ma. Ocean Drilling Program (ODP) Site 1051 is located in the North Atlantic and does not have a distinct record of the Carbon Isotope Excursion in the $\delta^{13}C$ record as is typically used for correlation purposes of this time interval, making it difficult to correlate to other sites such as Site 1267 in the South Atlantic. At both sites, however, a minimum in the $\delta^{34}S$ record was recorded and used to align the two records. Ages were determined by biostratigraphy.

S isotope data are becoming more widely available for many study locations and, as illustrated above, have the potential to become a more useful tool for stratigraphy and correlation as we refine the global S isotope record. The challenge in the next few years is to expand the available data to produce a reliable, high-resolution, secular data set of seawater S isotope values such that a high-resolution curve atleast like the one currently available for the past 130 Ma but ideally at even higher resolution could be produced and used for age determination.

REFERENCES

Algeo, T.J., Ellwood, B.B., Thoa, N.T.K., Rowe, H., Maynard, J.B., 2007. The Permian-Triassic boundary at Nhi Tao, Vietnam: Evidence for recurrent influx of sulfidic watermasses to a shallow-marine carbonate platform. Palaeogeography, Palaeoclimatology, Palaeoecology 252, 304–327.

Arthur, M.A., 2000. Volcanic contributions to the carbon and sulfur geochemical cycles and global change. In: Sigurdsson, H. (Ed.), Encyclopedia of Volcanoes. Academic Press, San Diego, pp. 1045–1056.

Ault, W., Jensen, M.L., 1963. A summary of sulfur isotope standards. In: Jensen, M.L. (Ed.), Biogeochemistry of Sulfur Isotopes. National Science Foundation Symposium Proceedings, Yale University, pp. 16–29.

Berner, R.A., 1999. Atmospheric oxygen over Phanerozoic time. PNAS 96, 10955–10957.

Berner, E.K., Berner, R.A., 1987. The Global Water Cycle: Geochemistry and Environment. Prentice-Hall, Englewood Cliffs, NJ, 397 pp.

Berner, R.A., Canfield, D.E., 1989. A new model for atmospheric oxygen over Phanerozoic time. American Journal of Science 289, 333–361.

Berner, R.A., Canfield, D.E., 1999. Atmospheric oxygen over Phanerozoic time. Proceedings of the National Academy of Sciences USA 96, 10955–10957.

Bottrell, S.H., Newton, R.J., 2006. Reconstruction of changes in global sulfur cycling from marine sulfate isotopes. Earth-Science Reviews 75, 59–83.

Burdett, J.W., Arthur, M.A., Richardson, M., 1989. A Neogene seawater sulfur isotope age curve from calcareous pelagic microfossils. Earth and Planetary Science Letters 94, 189–198.

Canfield, D.E., 2001. Isotope fractionation by natural populations of sulfate-reducing bacteria. Geochimica et Cosmochimica Acta 65, 1117–1124.

Canfield, D., Thamdrup, B., 1994. The production of ^{34}S-depleted sulfide during bacterial disproportionation of elemental sulfur. Science 266, 1973–1975.

Chiba, H., Sakai, H., 1985. Oxygen isotope exchange rate between dissolved sulfate and water at hydrothermal temperatures. Geochimica et Cosmochimica Acta 49 (4), 993–1000.

Claypool, G.E., Holser, W.T., Kaplan, I.R., Sakai, H., Zak, I., 1980. The age curves of sulfur and oxygen isotopes in marine sulfate and their mutual interpretation. Chemical Geology 28, 199–260.

Eagle, M., Paytan, A., Arrigo, K.R., van Dijken, G., Murray, R.W., 2003. A comparison between excess barium and barite as indicators of carbon export. Paleoceanography 18, 1–13.

Farquhar, J., Bao, H., Thiemens, M., 2000. Atmospheric influence of Earth's earliest sulfur cycle. Science 289, 756–758.

Goldhaber, M.B., Kaplan, I.R., 1974. The sulfur cycle. In: Goldberg, E.D. (Ed.), The Sea. 5. Marine Chemistry. Wiley, New York, pp. 569–655.

Gorjan, P., Kaiho, K., Kakegawa, T., Niitsuma, S., Chen, Z.Q., Kajiwara, Y., Nicora, A., 2007. Paleoredox, biotic and sulfur-isotopic changes associated with the end-Permian mass extinction in the western Tethys. Chemical Geology 244, 483–492.

Gray, E., 2007. Export Productivity and Sulfur Isotope Records over the Paleocene Eocene Thermal Maximum. Master's Thesis, Geological and Environmental Sciences, Stanford University, 126 pp.

Griffith, M.E., Paytan, A., 2012. Barite in the Ocean - Occurrence, Geochemistry and Paleoceanographic Applicators, Sedimentology. In Press.

Habicht, K.S., Canfield, D.E., Rethmeier, J., 1998. Sulfur isotope fractionation during bacterial reduction and disproportionation of thiosulfate and sulfite. Geochimica et Cosmochimica Acta 62, 2585–2595.

Harland, W.B., Armstrong, R.L., Cox, A.V., Craig, L.A., Smith, A.G., Smith, D.G., 1990. A geologic time scale 1989. Cambridge University Press, Cambridge, 263 pp.

Holser, W.T., Kaplan, I.R., 1966. Isotope geochemistry of sedimentary sulfates. Chemical Geology 1, 93–135.

Holser, W.T., Schidlowski, M., Mackenzie, F.T., Maynard, J.B., 1988. Geochemical cycles of carbon and sulfur. In: Gregor, C.B., Garrels, R.M., Mackenzie, F.T., Maynard, J.B. (Eds.), Chemical Cycles in the Evolution of the Earth. Wiley, New York, pp. 105–173.

Horita, J., Zimmermann, H., Holland, H.D., 2002. Chemical evolution of seawater during the Phanerozoic: Implications from the record of marine evaporites. Geochimica et Cosmochimica Acta 66, 3733–3756.

Kampschulte, A., Strauss, H., 2004. The sulfur isotopic evolution of Phanerozoic sea water based on the analysis of structurally substituted sulfate in carbonates. Chemical Geology 204, 255–286.

Kampschulte, A., Bruckschen, P., Strauss, H., 2001. The sulphur isotopic composition of trace sulphates in Carboniferous brachiopods: Implications for coeval seawater, correlation with other geochemical cycles and isotope stratigraphy. Chemical Geology 175, 149–173.

Kaplan, I.R., 1983. Stable isotopes of sulfur, nitrogen and deuterium in Recent marine environments. SEPM Short Course 10, 108.

Kaplan, I.R., 1983. Stable isotopes of sulfur, nitrogen and deuterium in recent marine environments. Stable Isotopes in Sedimentary Geology. In: Arthur, M.A., Anderson, T.F., Kaplan, I.R., Veizer, J., Land, L.S. (Eds.), Dallas: Soc. Econ. Paleontol. Mineral 2:1–108.

Kramm, U., Wedepohl, K.H., 1991. The isotopic composition of strontium and sulfur in seawater of Late Permian (Zechstein) age. Chemical Geology 90, 253–262.

Krouse, H.R., 1980. Sulphur isotopes in our environment. In: Fritz, P., Fontes, J.C. (Eds.), Handbook of Environmental Isotope Geochemistry. Elsevier, Amsterdam, pp. 435–471.

Lowenstein, T.K., Timofeeff, M.N., Brennan, S.T., Hardie, L.A., Demicco, R.V., 2001. Oscillations in Phanerozoic seawater chemistry: Evidence from fluid inclusions. Science 294, 1086–1088.

Lyons, T.W., Walter, L.M., Gellatly, A.M., Martini, A.M., Blake, R.E., 2004. Sites of anomalous organic remineralization in the carbonate sediments of South Florida, USA: The sulfur cycle and carbonate-associated sulfate. Geological Society of America Special Paper 379, 161–176.

McArthur, J.M., Howarth, R.J., Bailey, T.R., 2001. Strontium isotope stratigraphy: LOWESS Version 3. Best-fit line to the marine Sr-isotope curve for 0 to 509 Ma and accompanying look-up table for deriving numerical age. Journal of Geology 109, 155–169.

Misi, A., Kaufman, A.J., Veizer, J., Powis, K., Azmy, K., Boggiani, P.C., Gaucher, C., Teixeira, J.B.G., Sanches, A.L., Iyer, S.S., 2007. Chemostratigraphic correlation of Neoproterozoic successions in South America. Chemical Geology 237, 143–167.

Newton, R.J., Pevitt, E.L., Wignal, P.B., Bottrell, S.H., 2004. Large shifts in the isotopic composition of seawater sulphate across the Permo-Triassic boundary in northern Italy. Earth and Planetary Science Letters 218, 331–345.

Ohkouchi, N., Kawamura, K., Kajiwara, Y., Wada, E., Okada, M., Kanamatsu, T., Taira, A., 1999. Sulfur isotope records around Livello Bonarelli (Northern Apennines, Italy) black shale at the Cenomanian-Turonian boundary. Geology 27, 535–538.

Paytan, A., Kastner, M., Martin, E.E., Macdougall, J.D., Herbert, T., 1993. Marine barite as a monitor of seawater strontium isotope composition. Nature 366, 45–49.

Paytan, A., Kastner, M., Campbell, D., Thiemens, M.H., 1998. Sulfur isotope composition of Cenozoic seawater sulfate. Science 282, 1459–1462.

Paytan, A., Martínez-Ruiz, F., Eagle, M., Ivy, A., Wankel, S.D., 2004. Using sulfur isotopes in barite to elucidate the origin of high organic matter accumulation events in marine sediments. Sulfur Biogeochemistry, GSA Special Paper 379, 151–160.

Pokrovskii, B.G., Melezhik, V.A., Bujakaite, M.I., 2006. Carbon, oxygen, strontium, and sulfur isotopic compositions in late Precambrian rocks of the Patom Complex, central Siberia: Communication 2, Nature of carbonates with ultralow and ultrahigh $\delta^{13}C$ values. Lithology and Mineral Resources 41, 576–587.

Rees, C.E., 1970. The sulphur isotope balance of the ocean: An improved model. Earth and Planetary Science Letters 17, 366–370.

Rees, C.E., Jenkins, W.F., Monster, J., 1978. The sulphur isotopic composition of ocean water sulphate. Geochimica et Cosmochimica Acta 42, 377–382.

Scholle, P.A., 1995. Carbon and sulfur isotope stratigraphy of the Permian and adjacent intervals. In: Scholle, P.A., Peryt, T.M., Ulmer-Scholle, D.S. (Eds.), The Permian of Northern Pangea, 1. Springer-Verlag, Berlin, pp. 133–149.

Strauss, H., 1993. The sulfur isotopic record of Precambrian sulfates: New data and a critical evaluation of the existing record. Precambrian Research 63, 225–246.

Strauss, H., 1997. The isotopic composition of sedimentary sulfur through time. Palaeogeography, Palaeoclimatology, Palaeoecology 132, 97–118.

Strauss, H., 1999. Geological evolution from isotope proxy signals: Sulfur. Chemical Geology 161, 89–101.

Thode, H.G., Monster, J., 1965. Sulfur-isotope geochemistry of petroleum, evaporites, and ancient seas. American Association of Petroleum Geologists Memoir 4, 367–377.

Walter, M.R., Veevers, J.J., Calver, C.R., Gorjan, P., Hill, A.C., 2000. Dating the 840–544 Ma Neoproterozoic interval by isotopes of strontium, carbon, sulfur in seawater, and some interpretative models. Precambrian Research 100, 371–433.